ORIGINAL PAPER

Purification of Purple Sweet Potato Extract by Dead-End Filtration and Investigation of Membrane Fouling Mechanism

Zhenzhou Zhu[1] · Yan Liu[1] · Qingyan Guan[1] · Jingren He[1] · Gang Liu[1] · Shuyi Li[1] ·
Luhui Ding[2] · Michel Y. Jaffrin[3]

Abstract Pulsed ultrasound-assisted extraction with water was carried out to extract valuable compounds from purple sweet potato (PSP). Quality properties and dead-end filtration of PSP extract were investigated. Solutes concentration in PSP extract were 118.60 ± 2.83, 599.8 ± 8.28, and 0.72 ± 0.03 µg mL^{-1} for total protein, total polyphenol, and total anthocyanin, respectively. Filtration with PES 50 kDa membrane-augmented polyphenol purity from 83.4 % in extract to 99.6 %. A protein removal coefficient of 99 % was achieved. Resistance in series model and Hermia's model was applied to quantify filtration resistance and investigate fouling mechanism during filtration. Gel layer resistance was the most important for all three used membranes (PES 0.1 µm, PES 100 kDa, and PES 50 kDa). Fitting of experimental data by Hermia's model revealed that the most suitable fouling mechanism varied, cake layer model for PES 0.1 µm and PES 100 kDa membrane and intermediate blocking model for PES 50 kDa membrane. For the purpose of more efficient polyphenol production, advanced filtration modules, such as cross-flow and rotating disk filtration module, are expected.

✉ Zhenzhou Zhu
zhuzhenzhou19831@gmail.com; zhenzhouzhu@126.com

[1] College of Food Science and Engineering, Wuhan Polytechnic University, 430023 Wuhan, China

[2] EA 4297 TIMR (UTC/ESCOM), Centre de Recherche de Royallieu, Université de Technologie de Compiègne, B.P. 20529, 60205 Compiègne Cedex, France

[3] UMR 7338, Technological University of Compiegne, 60205 Compiegne Cedex, France

Introduction

Sweet potatoes crops are important for food and feed due to their richness in dietary fibers, minerals, vitamins, and antioxidants (Teow et al. 2007). Purple sweet potato (PSP) contains a high level of polyphenol and anthocyanin compared to those of white, yellow, or orange potatoes (Wang et al. 2011). It has been reported that the concentration of anthocyanin in PSP is similar to the highest anthocyanin production crops, such as blueberries, blackberries, cranberries, or grapes (Bridgers et al. 2010). Recent studies reported that compounds (polyphenol and anthocyanin) in PSP extract had many functional abilities, such as antioxidant (Zhang et al. 2010), hepato-protection (Hwang et al. 2011), and memory enhancing (Lu et al. 2012). Moreover, anthocyanins in PSP possess better heat stability compared to other sources of anthocyanin. Their structures are identified as mono-acylated or di-acylated forms of cyanidin and peonidin (Tiwari et al. 2009; Montilla et al. 2011). Since PSP is a low-cost crop, it may be a good source of natural polyphenol and anthocyanin for industrial production.

Currently, methanol and ethanol are the most commonly used solvents, for valuable compounds' (polyphenol and anthocyanin) extraction from PSP, due to their high extraction yield (Liu et al. 2013; Bridgers et al. 2010). However, the use of organic solvent is also considered toxic and hazardous to the environment. Thus, it is interesting to investigate anthocyanin and polyphenol extraction from PSP with water as solvent using extraction intensification methods (for example, ultrasound).

Like extracts from other plants (Sant'Anna et al. 2012), PSP extract contains a lot of impurities (mainly proteins), apart from target compounds (polyphenol and anthocyanin).

The existence of impurities restrains the function and application of target molecules. Thus, removal of impurities in PSP extract is important for PSP valorization.

Currently, membrane filtration has been widely used for the separation of valuable molecules from extracts with advantages of low operation cost, low-energy consumption, and no chemical agent addition (Namvar et al. 2013; Husson et al. 2013; Fuenmayor et al. 2014; Cassano et al. 2007; Pap et al. 2010). However, the application of filtration in industrial scale is limited by membrane fouling, which decreases filtration flux and restrains the productivity of filtration process (Zhu et al. 2014). Fouling formation and its effect on filtration are influenced by various parameters, such as trans-membrane pressure, solute size and physico-chemical properties, and feed and membrane characteristics.

Theories have been developed to understand fouling phenomenon and its mechanism in order to prevent fouling and increase filtration productivity. Previous investigation (de la Garza and Boulton 1984) proposed an exponential model, assuming that the total resistance to filtrate flow was empirically related to the filtrate volume. This exponential model was successfully used in filtration of soluble rice bran fiber, apple juice, chicory juice, and stevia extract to explain filtration behaviors (Wan et al. 2012; Zhu et al. 2013; Gokmen and Cetinkaya 2007; Reis et al. 2009). However, detailed information about fouling resistance and fouling mechanism identification was not given in this empirical model. For quantifying fouling resistance, a resistance in series model was proposed, assuming that total filtration resistance consisted of four major factors, membrane hydraulic resistance (R_m), concentration polarization resistance (R_c), cake or gel layer resistance (R_g), and adsorption resistance (R_a). The total fouling resistance was obtained by adding these four factors (Wang et al. 2012). Hermia (1982) developed a semi-empirical model to describe the fouling mechanism, in which four sub-models (complete blocking model, standard blocking model, intermediate blocking model, and the cake layer model) were included. This model permits to understand the main fouling mechanism.

The aim of this work is to study an ultrasound-assisted extraction of valuable compounds (such as polyphenols and anthocyanins) from PSP without adding organic solvent, to examine the separation of target molecules from PSP extract impurities, and to investigate filtration behavior and membrane fouling mechanism during filtration process.

Materials and Methods

Extraction

Extraction experiments were carried out at a solid/liquid ratio of 1:20, with 90 g of fresh PSP (purchased from a local market at Wuhan, China, and milled by a Joyoung cooker, type JYL-

D022, at a rotating speed of 20,000 rpm and a power of 250 W) and 1800 g of distilled water. Extraction tests were carried out with an ultrasonic processor FS-250N (Sonxi Ultrasonic Instrument, China) in pulsed mode (every 6 s treatment with a pause of 3 s). The treatment power was set at 150 W, and extraction temperature was set at 58±2 °C. The duration of extraction process was 1 h. In the extraction test, hydrochloric acid with a concentration of 4 % was added to obtain a pH in the extracted solvent of around 1, which is in the pH range of maximum anthocyanins color stability, in order to prevent the degradation of those compounds (Lapornik et al. 2005). The extract was centrifuged for 5 min at 6000g and prefiltered by a 200-mesh filter (with pore size of 74 μm) to remove pulps, then divided into portions, and stored at the temperature of −20 °C until further analysis and use.

Filtration of PSP Extract

Dead-end micro-filtration and ultra-filtration were performed in a self-fabricated filtration module (effective membrane area $3.03 \cdot 10^{-3}$ m^2 and maximal volume 250 mL) (Fig. 1). The aim was to separate proteins (obtained in retentate) from polyphenols and anthocyanins (obtained in permeate). For each experiment, 100 mL of PSP extract was used, and 60 mL of filtrate was obtained. Two types of polyethersulfone (PES) micro-filtration membranes (Ande membrane, China) with pore sizes of 0.3 and 0.1 μm and two types of PES ultra-filtration membranes (Microdyn-Nadir GmbH, Germany) with molecular weight cutoff (MWCO) of 100 and 50 kDa were used to purify PSP extract. A new membrane was used for each set of experiment. Filtration experiments were performed at room temperature, and the selected trans-membrane pressure (TMP) was 0.2 and 0.4 MPa. Permeate volume and filtration time were recorded for analysis.

Resistance in Series Model

In order to quantify membrane fouling, a resistance in series model was applied in this study. This model has been successfully used previously by other researchers in filtration of fermentation broth and enzyme membrane reactor (Wang et al. 2012; Luo et al. 2014a). According to this resistance in series model (Eq. 1), in dead-end filtration, flux decline can be explained by the total filtration resistance (R_t) including four terms: membrane hydraulic resistance (R_m), cake layer resistance (R_g), concentration polarization resistance (R_c), and adsorption resistance (R_a).

$$R_t = R_m + R_g + R_c + R_a = \frac{\Delta P}{\mu J} \qquad (1)$$

where J is the permeate flux (m^3/m^{2}s), $\triangle P$ is the transmembrane pressure (TMP, Pa), and μ is the dynamic
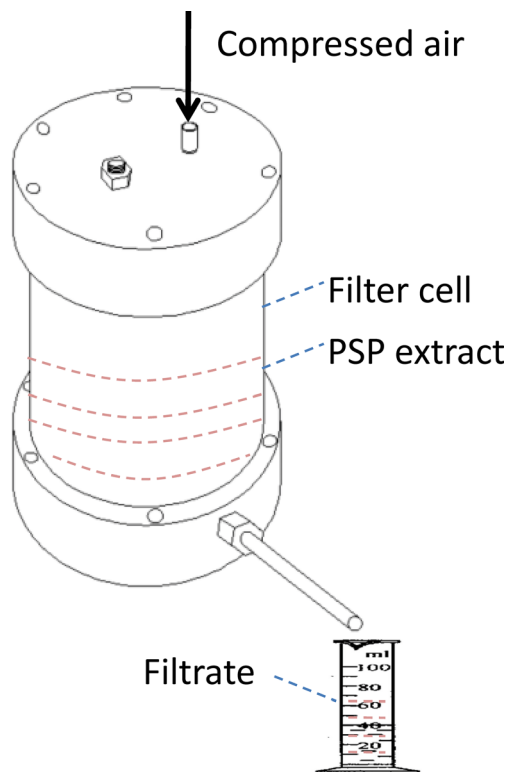
Fig. 1 Schematic diagram of the filtration setup

viscosity of permeate (Pa·s). All resistances (R_m, R_g, R_c and R_a) are in m^{-1}.

To determine all the resistances, the following procedure was adopted: First, the membrane hydraulic resistance R_m was calculated by measuring the flux of distilled water through a clean membrane (J_0). In this situation, R_c, R_g, and R_a were 0. Eq. (1) could be written as:

$$\frac{R_m P}{\mu J_0} \tag{2}$$

The PSP extract was filtrated, and the permeate flux (J) was recorded during the whole process. According to Eq. (1), R_t could be calculated during this process. Then, the feed PSP extract was replaced by distilled water, and the water flux in this situation, J_{pore}, was recorded. At this point, concentration polarization could be assumed to be 0 ($R_c = 0$) and R_m was already determined, so we have the sum of R_g and R_a:

$$R_a + R_g = \frac{\Delta P}{\mu_0 J_{pore}} - R_m \tag{3}$$

Then, the gel layer was removed by flushing the membrane with distilled water, and the water flux J_{irr} was measured. At this point, the concentration polarization resistance R_c and the gel or cake layer resistance R_g could be assumed to be 0. Therefore,

$$R_a = \frac{\Delta P}{\mu_0 J_{irr}} - R_m \tag{4}$$

After obtaining the value of R_a, R_g could be calculated from Eq. (3). Thus, all membrane resistances can be quantified by Eqs. (1)–(4).

Hermia's Model

Apart from quantification of membrane fouling by resistance in series model, identification of fouling mechanism provides another comprehensive method for understanding the flux decline. Hermia developed a semi-empirical model for dead-end filtration based on constant pressure condition in order to predict the fouling mechanism that governs the flux decline during the filtration. According to Hermia's model (Hermia 1982; Vela et al. 2008), there are four basic types of fouling: complete blocking model, intermediate blocking model, standard blocking model, and cake layer model. In Hermia's model (Eq. 5),

$$\frac{d^2 t}{dV^2} = k\left(\frac{dt}{dV}\right)^n \tag{5}$$

where t is filtration time (s), V is permeate volume (m^3), k is constant, and n can have different values, depending upon different types of fouling: $n=2$ for the complete blocking model, $n=1.5$ for the standard blocking model, $n=1$ for the intermediate blocking model, and $n=0$ for the cake layer model. By integrating Eq. (5), four linear equations can be obtained as follows:

For $n=2$:

$$\ln J = \ln J_0 - K_c t \tag{6}$$

For $n=1.5$:

$$\frac{1}{J^{0.5}} = \frac{1}{J_0^{0.5}} + K_s t \tag{7}$$

For $n=1$:

$$\frac{1}{J} = \frac{1}{J_0} + K_i t \tag{8}$$

For $n=0$

$$\frac{1}{J^2} = \frac{1}{J_0^2} + K_g t \tag{9}$$

where J is the permeate flux ($Lm^2 h^{-1}$), t is the filtration time (min), J_0 is the initial permeate flux when $t=0$, and K_c, K_s, K_i, and K_g are the model constants. The most likely fouling mechanisms can be deduced by fitting the experimental flux data using Eqs. (6)–(9) and comparing their regression coefficients.

Analysis of Extract and Filtrate

Total Polyphenol Content

Total polyphenol content (TP) was determined by Folin–Ciocalteu assay (Singleton et al. 1999). Folin–Ciocalteu reagent was prepared by our laboratory. Standard solutions of different concentrations from 0 to 0.1 mg/mL were made up using gallic acid. Portions of 1 ml sample, 1 mL Folin–Ciocalteu reagent, and 1.5 mL 20 % (w/v) Na$_2$CO$_3$ were added successively to a glass tube, then distilled water was added to increase the volume to 10 mL. The solution was placed in the dark for 2 h at room temperature. The last absorbance was measured at 760 nm. Total polyphenol (TP) was expressed as gallic acid equivalent (GAE).

Total Protein Content

The concentration of protein (TC) in extract and permeate was determined by Bradford method (Bradford 1976). One milliliter of sample and 5 mL of prepared Coomassie Brilliant Blue G-250 solution were added successively to a glass tube, then distilled water was added to increase the volume to 10 mL. After 5 min at room temperature, the last absorbance of solution was measured at 595 nm. Bovine serum albumin (BSA) was used as standard.

Total Anthocyanin Measurement

Total anthocyanin (TA) was determined according to a pH differential method based on color change of anthocyanin with pH (Lee et al. 2005). For each sample, the absorbance was measured at pH 1.0 and pH 4.5. The observed absorbance difference was proportional to anthocyanin content. TA content was calculated according to the following equation:

$$TAC(mg/L) = \frac{Abs}{\varepsilon L} \times MW \times D \times 1000 \tag{10}$$

with

$$Abs = (A_{541nm} - A_{700nm})pH_{1.0} - (A_{541nm} - A_{700nm})pH_{4.5} \tag{11}$$

where TA is the total anthocyanin content expressed as cyanidin-3-glucoside equivalent (CGE) (mg CGE/L), A_{541} and A_{700} are absorbances at 541 and 700 nm, respectively, MW is cyanidin-3-glucoside molecular weight (449.2 g/mol), D is the dilution factor, ε is cyanidin-3-glucoside molar absorptivity (26,900 L/mol/cm), L is the measurement cell path length (1 cm in the present study), and 10^3 is the conversion factor from g to mg.

Estimation of Filtration Efficiency and Data Analysis

Concentrations of protein (C_{pr}), polyphenol (C_{ph}), and anthocyanin (C_{an}) were measured in extract and filtrate samples. In order to evaluate the purification efficiency of filtration process, a modified purity towards protein (P_{pr}) was defined as:

$$P_{pr}(\%) = \frac{C_{pr}}{C_{pr} + C_{ph} + C_{an}} \times 100 \tag{12}$$

Purity towards polyphenol (P_{ph}) was defined as:

$$P_{ph}(\%) = \frac{C_{ph}}{C_{pr} + C_{ph} + C_{an}} \times 100 \tag{13}$$

Purity towards anthocyanin (P_{an}) was defined as:

$$P_{an}(\%) = \frac{C_{an}}{C_{pr} + C_{ph} + C_{an}} \times 100 \tag{14}$$

The purification efficiency of PSP extract was estimated using the value of relative removal of protein (R_{pr}) defined as:

$$R_{pr} = \frac{C_{pr}}{C_{pr_0}} \tag{15}$$

where C_{pr0} is the initial concentration of protein in PSP extract.

Polyphenol selectivity (S) of filtration was calculated as

$$S = \frac{TC_{ph}}{TC_{pr}} \tag{16}$$

where TC_{ph} and TC_{pr} are transmission coefficient of polyphenol and protein, respectively. They are defined as:

$$TC = \frac{C_f}{C_r} \tag{17}$$

where C_f and C_r are polyphenol and protein concentration in filtrate and retentate, respectively. The value of C_r was estimated as:

$$C_r = (C_0 V_0 - C_f V)/(V_0 - V_f) \tag{18}$$

where C_0 is the initial concentration of polyphenol (or protein), V_0 is the initial feed volume, and V_f is the filtrate volume.

Coefficients of rejection of proteins, RC_{pr}, anthocyanins, RC_{an}, and polyphenols, RC_{ph}, were estimated using the equation

$$RC = 1 - \frac{C_f}{C_r} \tag{19}$$

where C_f and C_r are solute (anthocyanins, polyphenols, or proteins) concentrations in the filtrate and retentate, respectively.

The recuperation yield of polyphenols (Y_{ph}) was calculated as:

$$Y_{ph} = \frac{C_{ph} \times V_f}{C_0 \times V_0} \quad (20)$$

Statistical Analysis

All the experiments were repeated, at least three times, and mean values and standard deviations were calculated. In the following figures, the values of error bars are equal to mean standard deviations.

Results and Discussion

Analysis of Extract Composition

The contents of total protein, total polyphenol, and total anthocyanin in the extract were 118.60±2.83, 599.8±8.28, and 0.72±0.03 µg mL^{-1}, respectively. These results confirmed that protein was the main impurity in PSP extract, where polyphenol and anthocyanin are target molecules. It should be noted that the yield of anthocyanin was only 1.44 mg/100 g fresh PSP, lower than anthocyanin extraction yield (~50 mg/100 g fresh PSP) from current applied extraction process with acidified ethanol solution (Puertolas et al. 2013). Other effective extraction intensification methods, such as pulsed electric fields and microwave treatment (Pap et al. 2012), are expected to realize efficient anthocyanin extraction without organic solvent for environmental protection and cost reduction. However, investigation of PSP extract obtained in this study is also considered interesting in view of polyphenol purification and understanding membrane fouling mechanism.

Filtrate Quality Analysis

Concentrations of proteins, polyphenols, and anthocyanins in the PSP extract and filtrate with different membranes were determined and presented in Fig. 2a. It is obvious that all three concentrations decreased with membrane pore size reduction due to molecule rejection caused by membrane and deposited layer. Concentration of protein decreased more significantly compared to that of polyphenol and anthocyanin. Thus, filtration may provide an efficient method for separation of protein from polyphenol and anthocyanin in PSP extract. The effect of TMP on solute concentration variation is also presented in Fig. 2. TMP increase led to solute concentration decrease, fast for protein concentration, and slowly for polyphenol and anthocyanin concentration; this may be explained by denser fouling layer formation at higher TMP. Also, it should be noted that the TMP-induced concentration difference was
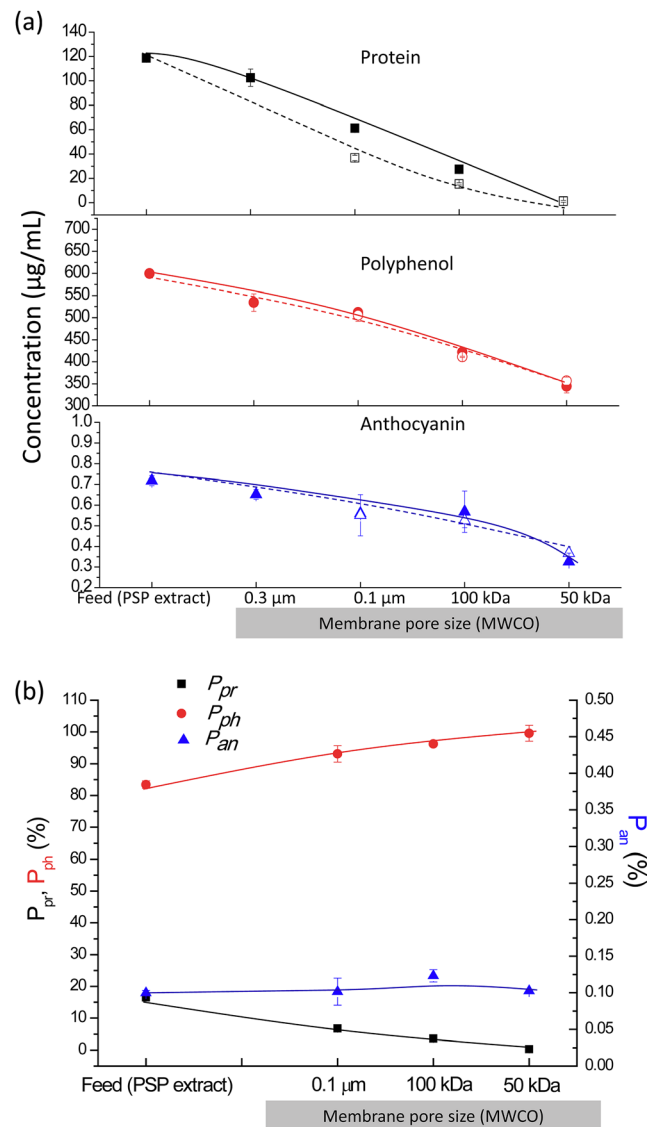

Fig. 2 **a** Evolution of concentration of proteins, polyphenols, and anthocyanins with membrane pore size or molecular weight cutoff (MWCO) at TMP of 0.2 MPa (*solid lines*) and 0.4 MPa (*dashed lines*). **b** Purity of protein (P_{pr}), polyphenol (P_{ph}), and anthocyanin (P_{an}) after filtration with different membrane at TMP of 0.4 MPa

small for membranes with low MWCO (for example, 50 kDa). For the purpose of well understanding concentration evolution, the coefficients of rejection for proteins, anthocyanins, and polyphenols were calculated and are presented in Table 1. As expected, membranes with smaller pore sizes led to higher coefficients of rejection for all three investigated solutes. Moreover, with the same membrane, higher TMP resulted in higher coefficient of rejection due to denser fouling layer. It should be noted that, with 50 kDa membrane, coefficients of rejection for proteins were bigger than 99 %, evidencing the purification function of membrane filtration.

For the purpose of comparing filtration efficiency in solute separation, the purities of solutes in filtrate were calculated and are presented in Fig. 2b. As expected, protein purity

Table 1 Coefficients of rejection (RC) of solutes at different filtration conditions

RC (%)	Membrane pore size (or MWCO) and TMP						
	0.3 μm	0.1 μm		100 kDa		50 kDa	
	0.2 MPa	0.2 MPa	0.4 MPa	0.2 MPa	0.4 MPa	0.2 MPa	0.4 MPa
RC_{pr}	28.21±0.90	70.06±2.52	84.74±3.98	89.23±3.75	94.33±2.74	99.53±3.68	99.61±4.28
RC_{an}	20.41±0.84	41.48±1.78	43.10±1.34	39.82±1.23	47.72±2.20	75.08±3.30	70.47±2.89
RC_{ph}	23.54±0.82	30.14±0.75	31.80±1.18	51.41±1.49	53.44±1.87	65.03±2.15	63.11±2.65

RC_{pr} coefficient of rejection of proteins, RC_{an} coefficient of rejection of anthocyanins, RC_{ph} coefficient of rejection of polyphenols

decreased, from 16.5 to 0.3 %, with membrane pore size reduction, while that of polyphenol increased (from 83.4 to 99.6 %) and anthocyanin (with a molecular weight of ~1 kDa; Lu et al. 2011) remained a purity of ~0.1 %. Based on membrane separation mechanism, we could assume that, although molecular size distribution is wide for each solute, in PSP extract, most proteins have larger molecular size than polyphenol and anthocyanin. Thus, the goal for separating protein and polyphenol in this study is confirmed by the results of Fig. 2. However, the recuperation yield of polyphenols in this study was not desirable due to small volume reduction ratio (2.5) and strong fouling; for example, Y_{ph} was only 34.41 ±1.62 % with a membrane of 50 kDa and a TMP of 0.2 MPa. Higher recuperation yield may be achieved by application of dia-filtration in cross-flow mode.

The effect of membrane pore size on relative removal of protein is presented in Fig. 3a. The value of relative removal percentage of protein augmented with membrane pore size reduction. This result was in accordance with the protein concentration evolution during filtration with different membranes. Figure 3a shows that the influence of TMP on protein removal was not significant for membranes with small MWCO. Especially when a PES 50 kDa membrane was used, no difference of protein removal could be observed for filtration at 0.2 and 0.4 MPa. This may be explained that the porosity and the fouling layer, which dominate the filtration process of 50 kDa membranes, were similar for filtrations under these two TMP. However, the dependence of polyphenol selectivity (S) on membrane pore size and TMP in Fig. 3b confirmed that both membrane pore size reduction and TMP increase enhanced polyphenol selectivity. It is interesting to note that, unlike protein removal, for a 50-kDa membrane, TMP increase (from 0.2 to 0.4 MPa) still enhanced polyphenol selectivity, facilitating purification of polyphenol in PSP extract.

Filtration Behavior and Membrane Fouling Analysis

Filtration Behavior Analysis

Filtrate volume versus filtration time is presented in Fig. 4. Since the filtration with PES 0.3 μm membrane was too fast to

allow us to accumulate sufficient data, filtration behavior analysis was only carried out for filtration with 0.1 μm and 100 and 50 kDa membrane. The effect of TMP was positive for 50 kDa membrane (Fig. 4a). For example, 13,000 s was required to obtain 30 mL of filtrate at 0.2 MPa, while 2000 s was sufficient when TMP increased to 0.4 MPa. However, the positive effect of TMP was slight for 100 kDa and 0.1 μm
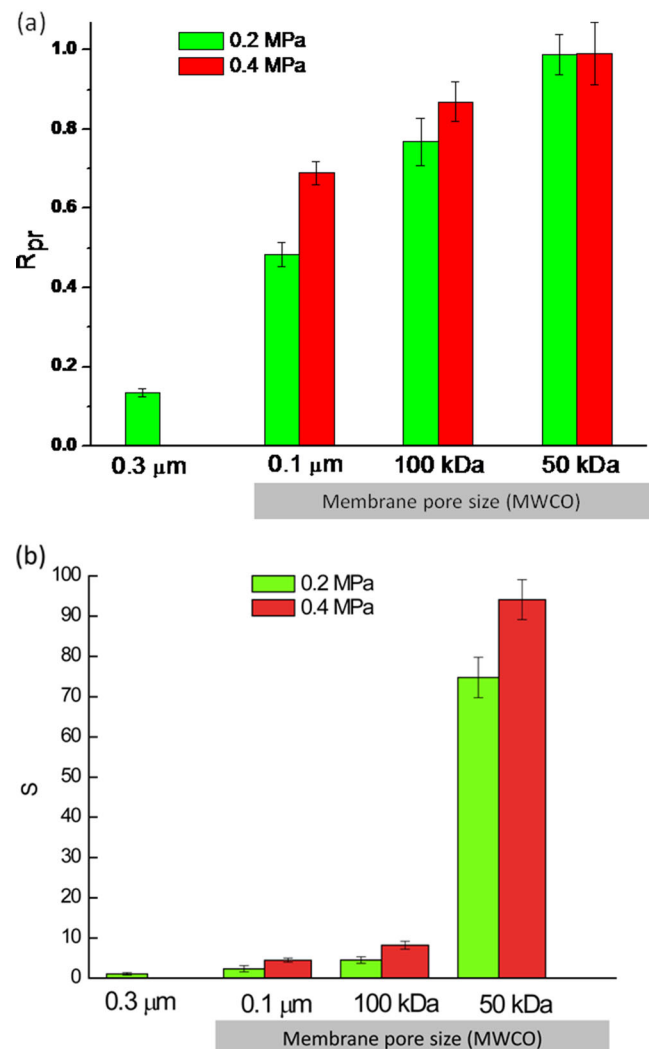

Fig. 3 a Relative removal of proteins during filtration and **b** variation of polyphenols selectivity during filtration with different membranes
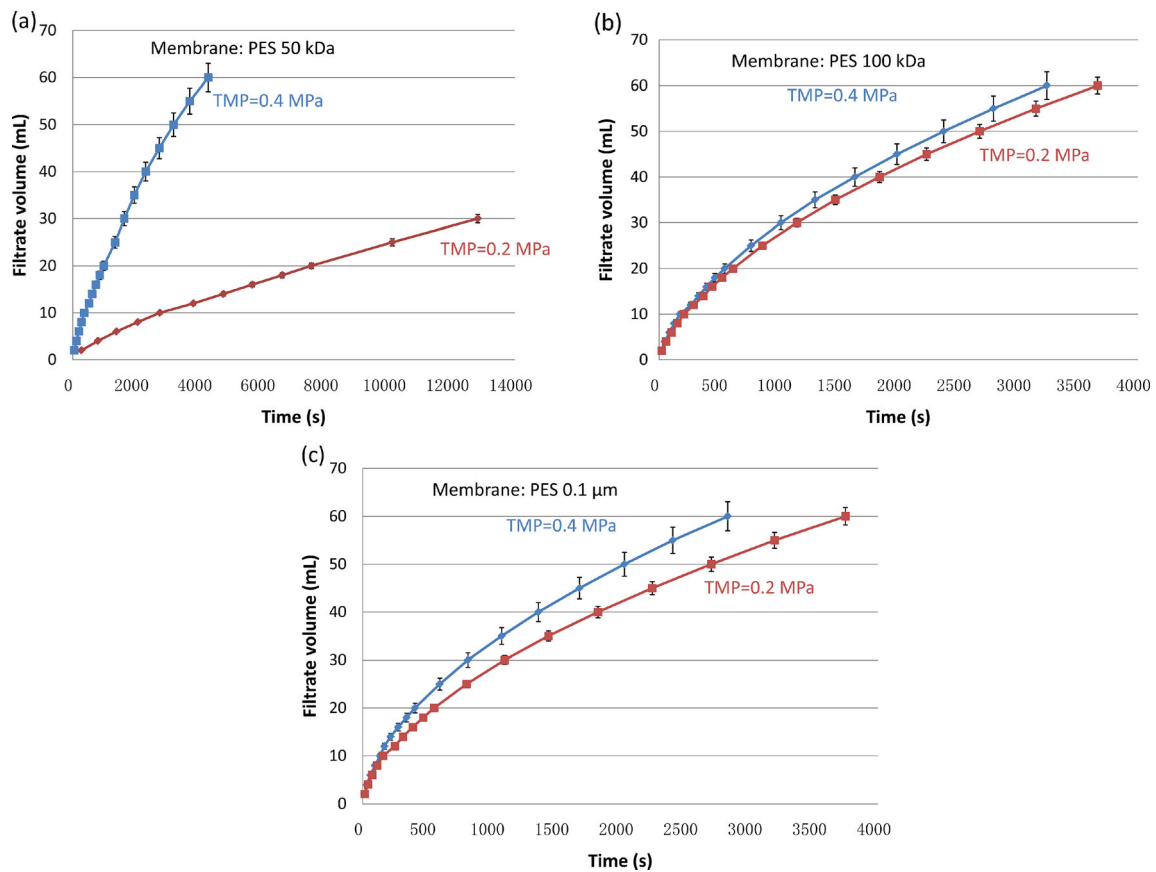
Fig. 4 Filtrate volume versus filtration time for membranes of 50 kDa (**a**), 100 kDa (**b**), and 0.1 μm (**c**)

membrane (Fig. 4b, c). The same tendency was also observed for initial flux of filtration at investigated conditions (Table 2). This may be explained by the rise of resistance and driving force when TMP increases. According to Bacchin et al. (2006), there exists an anti-fouling effect during unstirred filtration: Brownian diffusion (back diffusion of rejected particles into the bulk, mainly due to the resulting concentration gradient). The Brownian diffusion coefficient is inversely proportional to particle size (Belfort et al. 1994). When applied TMP is under the required TMP for threshold flux of membrane, the polarized layer on membrane is dynamic and most rejected particles near membrane surface are floating, inducing an almost constant filtration resistance. Thus, the driving force will increase when TMP rises. However, for another used membrane, if TMP exceeds the required value for threshold flux, more retained

particles may assemble together, leading to a more compacted fouling layer. The Brownian diffusion of aggregated particles seriously decreases, and more particles accumulate and deposit on the membrane, causing a significant augmentation of fouling resistance, which overcomes the benefit of driving force caused by TMP increase. According to Luo et al. (2014b), the threshold flux decreased with membrane pore size augmentation. Thus, for a 50-kDa membrane, TMP increase acted as driving force, while for 100 kDa and 0.1 μm membranes, fouling resistance augmentation was more important when TMP increased.

Resistance in Series Analysis

In order to analyze resistances that lead to flux decline during the filtration process, a resistance in series model was applied

Table 2 Initial flux of filtration (J_0) at different conditions

Initial flux Lm^{-2} h^{-1}	Membrane pore size (or MWCO) and TMP					
	0.1 μm		100 kDa		50 kDa	
	0.2 MPa	0.4 MPa	0.2 MPa	0.4 MPa	0.2 MPa	0.4 MPa
J_0	138.91±4.55	179.47±6.42	99.67±4.37	111.88±4.52	8.51±3.78	44.68±2.69

J_0 was defined as average flux to accumulate the first 2 mL permeate

Table 3 Fouling resistance for different membranes

Membrane	Resistance ($\times 10^{13}$ m^{-1}) (%)				
	R_t	R_m	R_c	R_g	R_a
PES 0.1 μm	10.3	0.03 (0.50)	4.62 (44.85)	5.60 (54.37)	0.04 (0.5)
PES 100 kDa	10.8	0.31 (2.85)	4.33 (40.09)	5.62 (52.04)	0.54 (5.00)
PES 50 kDa	14.1	2.01 (14.26)	4.72 (33.48)	5.22 (37.02)	2.15 (15.25)

in this study. Fouling resistances for different membranes are presented in Table 3. As expected, the membrane hydraulic resistance of PES 50 kDa membrane was the most important compared to other two membranes. Filtration resistance analysis showed that formation of gel layer and concentration polarization were two major reasons for flux decline. Since filtration processes were carried out without stirring, gel layer-induced cake resistance was the most important. It should be noted that the ratio R_g/R_t increased with membrane pore size, 37 and 54 % for PES 50 kDa and PES 0.1 μm membranes, respectively, while the ratio R_a/R_t decreased when membrane pore size increased. Two explanations may be applicable for this result. The one is that foulants in membranes with bigger pores were easier to be cleaned up by the "washing" effect of higher water flux, and the other is that the pores are less accessible due to the gel layer formation.

Hermia's Model Analysis

Hermia's models were used to investigate the fouling mechanism of each membrane during filtration by fitting experimental data with experimental data. Figure 5 represents the fitting of experimental data to four types of Hermia's models according to Eqs. (6)–(9). Table 4 showed all corresponding correlation coefficients (R^2), and an asterisk on R^2 values indicated the besting fitting model. Results showed that experimental data of PES 100 kDa and PES 0.1 μm membranes were best fitted to the cake layer model, showing that cake layer formation was the dominant fouling mechanism. In this situation, molecules bigger than membrane pores accumulated on the membrane surface and formed a permeable cake layer. However, the fouling of PES 50 kDa was dominated by intermediate blocking mechanism. In this situation, molecules that
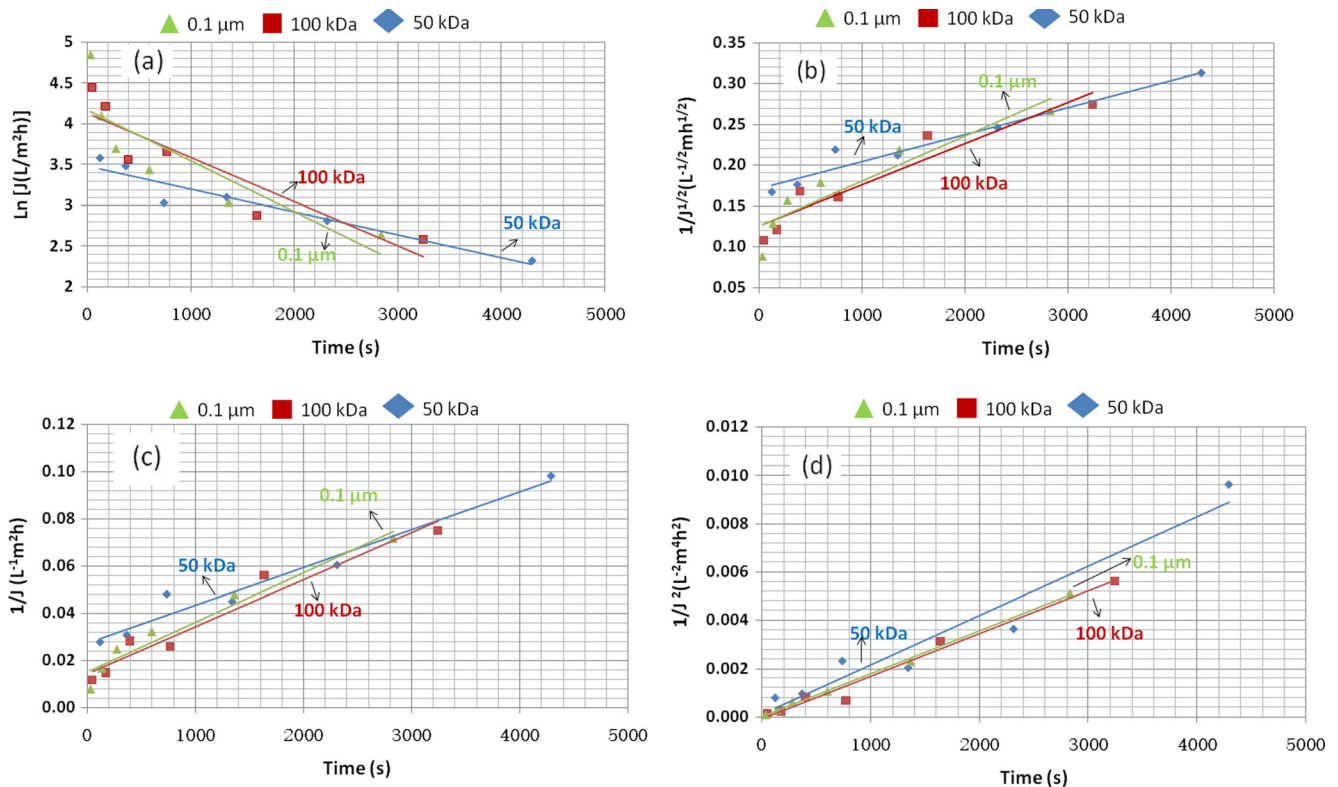

Fig. 5 Fitting of experimental data to the complete blocking model (**a**), standard blocking model (**b**), intermediate blocking model (**c**), and cake layer model (**d**)

Table 4 Coefficient (R^2) of linear regression of fitting experimental data according to filtration blocking model for different membranes

Membrane	Complete blocking	Standard blocking	Intermediate blocking	Cake layer
PES 50 kDa	0.9150	0.9515	0.9629[*]	0.9388
PES 100 kDa	0.8280	0.9008	0.9453	0.9781*
PES 0.1 μm	0.7270	0.8645	0.9530	0.9977*

*Indicates the best fitting model of membrane in that row

reached the pore entrance blocked the pore, but not all molecules reaching membrane surface could seal separate membrane pores. Different fouling mechanisms confirmed that foulants in big membrane pores could be wiped off by filtration flux, as mentioned in "Resistance in Series Analysis." Also, results of Table 4 are consistent with those of Table 2, showing that adsorption resistance of PES 50 kDa membrane (15 %) was greater than that of PES 100 kDa (5 %) and PES 0.1 μm membrane (1 %).

Although best fittings of each membrane for four fouling mechanisms were indicated, we should also note that for PES 50 kDa membrane, the value of R^2 was greater than 0.9 for different fouling mechanisms. This may be caused by the complex influence of multiple factors (feed composition, interaction between membrane pore size and molecular in feed, and membrane material), leading to combined fouling mechanism during filtration (Bolton et al. 2006). This assumption could be evidenced by the fitting of experimental data with Hermia's model using $\frac{d^2t}{dV^2} = k\left(\frac{dt}{dV}\right)^n$ (Fig. 6). As shown in Fig. 6, the value of n were 1.48, 0.81, and 0.96 for 50 kDa, 100 kDa, and 0.1 μm membrane respectively. These results confirmed the combined fouling during filtration of PSP extract.

Conclusions

Purple sweet potato (PSP) extract was prepared by ultrasound-assisted extraction with water as solvent. Dead-end filtration
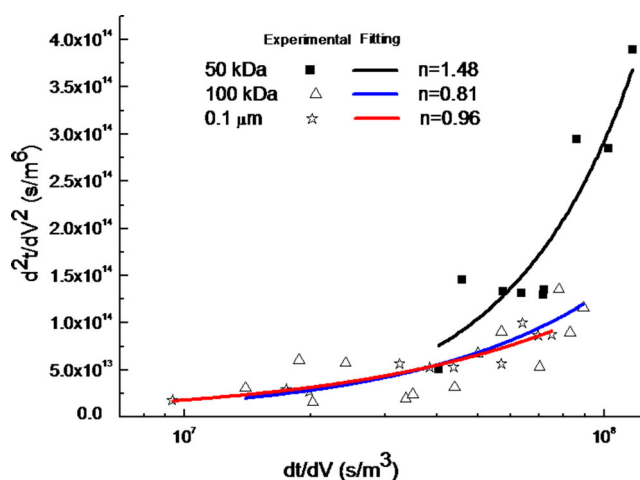
without stirring was applied to separate impurity (protein) and target molecules (polyphenol and anthocyanin) in PSP extract. Extract and filtrate analysis revealed that compared to PSP extract (with a proteins purity of 16.5 % and polyphenols purity of 83.4 %), the purity of protein decreased to 3.2 %, while that of polyphenol increased to 99.6 % after filtration using a PES 50 kDa membrane at 0.4 MPa. Anthocyanin purity remained at a level of ~0.1 %. However, due to low anthocyanin concentration (0.72 μg mL^{-1}) in the extract, separation of polyphenol and protein by filtration seemed more important in this study. Other effective extraction intensification methods, such as pulsed electric fields and microwave treatment, are expected to realize efficient anthocyanin extraction without organic solvent. The results of protein removal and polyphenol selectivity revealed that membrane pore size reduction had a positive influence on protein removal and polyphenol purification. The investigation of filtration behavior showed that the effect of TMP on filtrate rate was more significant for the PES 50 kDa membrane than PES 0.1 μm and PES 100 kDa membranes. Resistance in series model and Hermia's model was applied to quantify fouling resistance and investigate fouling mechanism during filtration. For all three studied membranes (PES 0.1 μm, PES 100 and PES 50 kDa), the resistance caused by formation of gel layer accounted for most of filtration resistance. However, the most suitable fouling mechanism was intermediate blocking for PES 50 kDa membrane and cake layer for PES 0.1 μm and PES 100 kDa by fitting of experimental data with Hermia's model. More efficient filtration with satisfactory filtrate purity can be expected if cross-flow and rotating disk filtration modules are applied.

Fig. 6 Fitting of experimental data with Hermia's model using equation $\frac{d^2t}{dV^2} = k\left(\frac{dt}{dV}\right)^n$

References

Bacchin, P., Aimar, P., & Field, R. W. (2006). Critical and sustainable fluxes: theory, experiments and applications. *Journal of Membrane Science, 281*(1–2), 42–69.

Belfort, G., Davis, R. H., & Zydney, A. L. (1994). The behavior of suspensions and macromolecular solutions in crossflow microfiltration. *Journal of Membrane Science, 96*(1), 1–58.

Bolton, G., Lacasse, D., & Kuriyel, R. (2006). Combined models of membrane fouling: development and application to microfiltration and ultrafiltration of biological fluids. *Journal of Membrane Science, 277*(1–2), 75–84.

Bradford, M. M. (1976). A rapid and sensitive method for the quantitation of microgram quantities of protein utilizing the principle of protein-dye binding. *Analytical Biochemistry, 72*(1), 248–254.

Bridgers, E. N., Chinn, M. S., & Truong, V.-D. (2010). Extraction of anthocyanins from industrial purple-fleshed sweet potatoes and enzymatic hydrolysis of residues for fermentable sugars. *Industrial Crops and Products, 32*(3), 613–620.

Cassano, A., Donato, L., & Drioli, E. (2007). Ultrafiltration of kiwifruit juice: operating parameters, juice quality and membrane fouling. *Journal of Food Engineering, 79*(2), 613–621.

de la Garza, F., & Boulton, R. (1984). The modeling of wine filtrations. *American Journal of Enology and Viticulture, 35*(4), 189–195.

Fuenmayor, C. A., Lemma, S. M., Mannino, S., Mimmo, T., & Scampicchio, M. (2014). Filtration of apple juice by nylon nanofibrous membranes. *Journal of Food Engineering, 122*, 110–116.

Gokmen, V., & Cetinkaya, O. (2007). Effect of pretreatment with gelatin and bentonite on permeate flux and fouling layer resistance during apple juice ultrafiltration. *Journal of Food Engineering, 80*(1), 300–305.

Hermia, J. (1982). Constant pressure blocking filtration laws—application to power-law non-Newtonian fluids. *Chemical Engineering Research and Design, 60a*, 183–187.

Husson, E., Araya-Farias, M., Gagné, A., & Bazinet, L. (2013). Selective anthocyanins enrichment of cranberry juice by electrodialysis with filtration membrane: influence of membranes characteristics. *Journal of Membrane Science, 448*, 114–124.

Hwang, Y. P., Choi, J. H., Choi, J. M., Chung, Y. C., & Jeong, H. G. (2011). Protective mechanisms of anthocyanins from purple sweet potato against tert-butyl hydroperoxide-induced hepatotoxicity. *Food and Chemical Toxicology, 49*(9), 2081–2089.

Lapornik, B., Prošek, M., & Golc Wondra, A. (2005). Comparison of extracts prepared from plant by-products using different solvents and extraction time. *Journal of Food Engineering, 71*(2), 214–222.

Lee, J., Durst, R. W., & Wrolstad, R. E. (2005). Determination of total monomeric anthocyanin pigment content of fruit juices, beverages, natural colorants, and wines by the pH differential method: collaborative study. *Journal of AOAC International, 88*(5), 1269–1278.

Liu, X., Mu, T., Sun, H., Zhang, M., & Chen, J. (2013). Optimisation of aqueous two-phase extraction of anthocyanins from purple sweet potatoes by response surface methodology. *Food Chemistry, 141*(3), 3034–3041.

Lu, J., Wu, D. M., Zheng, Y. L., Hu, B., Cheng, W., & Zhang, Z. F. (2012). Purple sweet potato color attenuates domoic acid-induced cognitive deficits by promoting estrogen receptor-alpha-mediated mitochondrial biogenesis signaling in mice. *Free Radical Biology and Medicine, 52*(3), 646–659.

Lu, Y., Li, J.-Y., Luo, J., Li, M.-L., & Liu, Z.-H. (2011). Preparative separation of anthocyanins from purple sweet potatoes by high-speed counter-current chromatography. *Chinese Journal of Analytical Chemistry, 39*(6), 851–856.

Luo, J., Meyer, A. S., Jonsson, G., & Pinelo, M. (2014a). Enzyme immobilization by fouling in ultrafiltration membranes: impact of membrane configuration and type on flux behavior and biocatalytic conversion efficacy. *Biochemical Engineering Journal, 83*, 79–89.

Luo, J., Morthensen, S. T., Meyer, A. S., & Pinelo, M. (2014b). Filtration behavior of casein glycomacropeptide (CGMP) in an enzymatic membrane reactor: fouling control by membrane selection and threshold flux operation. *Journal of Membrane Science, 469*, 127–139.

Montilla, E. C., Hillebrand, S., & Winterhalter, P. (2011). Anthocyanins in purple sweet potato (Ipomoea batatas L.) varieties. *Fruit, Vegetable and Cereal Science and Biotechnology, 5*(2), 19–23.

Namvar, A., Haq, I., Shields, M., Amoako, K. K., & Warriner, K. (2013). Extraction of Bacillus endospores from water, apple juice concentrate, raw milk and lettuce rinse solutions using tangential flow filtration. *Food Control, 32*(2), 632–637.

Pap, N., Beszédes, S., Pongrácz, E., Myllykoski, L., Gábor, M., Gyimes, E., Hodúr, C., & Keiski, R. L. (2012). Microwave-assisted extraction of anthocyanins from black currant marc. *Food and Bioprocess Technology, 6*(10), 2666–2674.

Pap, N., Mahosenaho, M., Pongrácz, E., Mikkonen, H., Jaakkola, M., Virtanen, V., Myllykoski, L., Horváth-Hovorka, Z., Hodúr, C., Vatai, G., & Keiski, R. L. (2010). Effect of ultrafiltration on anthocyanin and flavonol content of black currant Juice (Ribes nigrum L.). *Food and Bioprocess Technology, 5*(3), 921–928.

Puertolas, E., Cregenzan, O., Luengo, E., Alvarez, I., & Raso, J. (2013). Pulsed-electric-field-assisted extraction of anthocyanins from purple-fleshed potato. *Food Chemistry, 136*(3–4), 1330–1336.

Reis, M. H. M., Da Silva, F. V., Andrade, C. M. G., Rezende, S. L., Maciel, M. R. W., & Bergamasco, R. (2009). Clarification and purification of aqueous stevia extract using membrane separation process. *Journal of Food Process Engineering, 32*(3), 338–354.

Sant'Anna, V., Marczak, L. D. F., & Tessaro, I. C. (2012). Kinetic modeling of anthocyanin extraction from grape marc. *Food and Bioprocess Technology, 6*(12), 3473–3480.

Singleton, V.L., Orthofer, R. & Lamuela-Raventós, R.M. (1999). Analysis of total phenols and other oxidation substrates and antioxidants by means of Folin-Ciocalteu reagent. *Methods in Enzymology*, vol 299, doi: 10.1016/S0076-6879(99)99017-1

Teow, C. C., Truong, V.-D., McFeeters, R. F., Thompson, R. L., Pecota, K. V., & Yencho, G. C. (2007). Antioxidant activities, phenolic and β-carotene contents of sweet potato genotypes with varying flesh colours. *Food Chemistry, 103*(3), 829–838.

Tiwari, B., O'Donnell, C., & Cullen, P. (2009). Effect of sonication on retention of anthocyanins in blackberry juice. *Journal of Food Engineering, 93*(2), 166–171.

Vela, M., Blanco, S. Á., García, J. L., & Rodríguez, E. B. (2008). Analysis of membrane pore blocking models applied to the ultrafiltration of PEG. *Separation and Purification Technology, 62*(3), 489–498.

Wan, Y. T., Prudente, A., & Sathivel, S. (2012). Purification of soluble rice bran fiber using ultrafiltration technology. *LWT–Food Science and Technology, 46*(2), 574–579.

Wang, C., Li, Q., Tang, H., Yan, D., Zhou, W., Xing, J., & Wan, Y. (2012). Membrane fouling mechanism in ultrafiltration of succinic acid fermentation broth. *Bioresource Technology, 116*, 366–371.

Wang, S.-M., Yu, D.-J., & Song, K. B. (2011). Quality characteristics of purple sweet potato (Ipomoea batatas) slices dehydrated by the addition of maltodextrin. *Horticulture, Environment, and Biotechnology, 52*(4), 435–441.

Zhang, Z. F., Lu, J., Zheng, Y. L., Hu, B., Fan, S. H., Wu, D. M., Zheng, Z. H., Shan, Q., & Liu, C. M. (2010). Purple sweet potato color protects mouse liver against d-galactose-induced apoptosis via inhibiting caspase-3 activation and enhancing PI3K/Akt pathway. *Food and Chemical Toxicology, 48*(8–9), 2500–2507.

Zhu, Z., Bals, O., Grimi, N., Ding, L., & Vorobiev, E. (2013). Qualitative characteristics and dead-end ultrafiltration of chicory juice obtained from pulsed electric field treated chicories. *Industrial Crops and Products, 46*, 8–14.

Zhu, Z., Mhemdi, H., Ding, L., Bals, O., Jaffrin, M.Y., Grimi, N. & Vorobiev, E. (2014). Dead-end dynamic ultrafiltration of juice expressed from electroporated sugar beets. *Food and Bioprocess Technology*.